Study of the baryonic B decay $B^- \rightarrow \Sigma_c^{++} \bar{p} \pi^- \pi^-$

J. P. Lees,[1] V. Poireau,[1] V. Tisserand,[1] J. Garra Tico,[2] E. Grauges,[2] A. Palano,[3a,3b] G. Eigen,[4] B. Stugu,[4] D. N. Brown,[5]
L. T. Kerth,[5] Yu. G. Kolomensky,[5] G. Lynch,[5] H. Koch,[6] T. Schroeder,[6] D. J. Asgeirsson,[7] C. Hearty,[7] T. S. Mattison,[7]
J. A. McKenna,[7] R. Y. So,[7] A. Khan,[8] V. E. Blinov,[9] A. R. Buzykaev,[9] V. P. Druzhinin,[9] V. B. Golubev,[9] E. A. Kravchenko,[9]
A. P. Onuchin,[9] S. I. Serednyakov,[9] Yu. I. Skovpen,[9] E. P. Solodov,[9] K. Yu. Todyshev,[9] A. N. Yushkov,[9] M. Bondioli,[10]
D. Kirkby,[10] A. J. Lankford,[10] M. Mandelkern,[10] H. Atmacan,[11] J. W. Gary,[11] F. Liu,[11] O. Long,[11] G. M. Vitug,[11]
C. Campagnari,[12] T. M. Hong,[12] D. Kovalskyi,[12] J. D. Richman,[12] C. A. West,[12] A. M. Eisner,[13] J. Kroseberg,[13]
W. S. Lockman,[13] A. J. Martinez,[13] B. A. Schumm,[13] A. Seiden,[13] D. S. Chao,[14] C. H. Cheng,[14] B. Echenard,[14]
K. T. Flood,[14] D. G. Hitlin,[14] P. Ongmongkolkul,[14] F. C. Porter,[14] A. Y. Rakitin,[14] R. Andreassen,[15] Z. Huard,[15]
B. T. Meadows,[15] M. D. Sokoloff,[15] L. Sun,[15] P. C. Bloom,[16] W. T. Ford,[16] A. Gaz,[16] U. Nauenberg,[16] J. G. Smith,[16]
S. R. Wagner,[16] R. Ayad,[17,*] W. H. Toki,[17] B. Spaan,[18] K. R. Schubert,[19] R. Schwierz,[19] D. Bernard,[20] M. Verderi,[20]
P. J. Clark,[21] S. Playfer,[21] D. Bettoni,[22a] C. Bozzi,[22a] R. Calabrese,[22a,a22b] G. Cibinetto,[22a,a22b] E. Fioravanti,[22a,a22b]
I. Garzia,[22a,a22b] E. Luppi,[22a,a22b] M. Munerato,[22a,a22b] M. Negrini,[22a,a22b] L. Piemontese,[22a] V. Santoro,[22a]
R. Baldini-Ferroli,[23] A. Calcaterra,[23] R. de Sangro,[23] G. Finocchiaro,[23] P. Patteri,[23] I. M. Peruzzi,[23,†] M. Piccolo,[23]
M. Rama,[23] A. Zallo,[23] R. Contri,[24a,24b] E. Guido,[24a,24b] M. Lo Vetere,[24a,24b] M. R. Monge,[24a,24b] S. Passaggio,[24a]
C. Patrignani,[24a,24b] E. Robutti,[24a] B. Bhuyan,[25] V. Prasad,[25] C. L. Lee,[26] M. Morii,[26] A. J. Edwards,[27] A. Adametz,[28]
U. Uwer,[28] H. M. Lacker,[29] T. Lueck,[29] P. D. Dauncey,[30] P. K. Behera,[31] U. Mallik,[31] C. Chen,[32] J. Cochran,[32]
W. T. Meyer,[32] S. Prell,[32] A. E. Rubin,[32] A. V. Gritsan,[33] Z. J. Guo,[33] N. Arnaud,[34] M. Davier,[34] D. Derkach,[34]
G. Grosdidier,[34] F. Le Diberder,[34] A. M. Lutz,[34] B. Malaescu,[34] P. Roudeau,[34] M. H. Schune,[34] A. Stocchi,[34] G. Wormser,[34]
D. J. Lange,[35] D. M. Wright,[35] C. A. Chavez,[36] J. P. Coleman,[36] J. R. Fry,[36] E. Gabathuler,[36] D. E. Hutchcroft,[36]
D. J. Payne,[36] C. Touramanis,[36] A. J. Bevan,[37] F. Di Lodovico,[37] R. Sacco,[37] M. Sigamani,[37] G. Cowan,[38] D. N. Brown,[39]
C. L. Davis,[39] A. G. Denig,[40] M. Fritsch,[40] W. Gradl,[40] K. Griessinger,[40] A. Hafner,[40] E. Prencipe,[40] R. J. Barlow,[41,‡]
G. Jackson,[41] G. D. Lafferty,[41] E. Behn,[42] R. Cenci,[42] B. Hamilton,[42] A. Jawahery,[42] D. A. Roberts,[42] C. Dallapiccola,[43]
R. Cowan,[44] D. Dujmic,[44] G. Sciolla,[44] R. Cheaib,[45] D. Lindemann,[45] P. M. Patel,[45,§] S. H. Robertson,[45] P. Biassoni,[46a,46b]
N. Neri,[46a] F. Palombo,[46a,46b] S. Stracka,[46a,46b] L. Cremaldi,[47] R. Godang,[47,‖] R. Kroeger,[47] P. Sonnek,[47] D. J. Summers,[47]
X. Nguyen,[48] M. Simard,[48] P. Taras,[48] G. De Nardo,[49a,49b] D. Monorchio,[49a,49b] G. Onorato,[49a,49b] C. Sciacca,[49a,49b]
M. Martinelli,[50] G. Raven,[50] C. P. Jessop,[51] J. M. LoSecco,[51] W. F. Wang,[51] K. Honscheid,[52] R. Kass,[52] J. Brau,[53] R. Frey,[53]
N. B. Sinev,[53] D. Strom,[53] E. Torrence,[53] E. Feltresi,[54a,54b] N. Gagliardi,[54a,54b] M. Margoni,[54a,54b] M. Morandin,[54a]
M. Posocco,[54a] M. Rotondo,[54a] G. Simi,[54a] F. Simonetto,[54a,54b] R. Stroili,[54a,54b] S. Akar,[55] E. Ben-Haim,[55] M. Bomben,[55]
G. R. Bonneaud,[55] H. Briand,[55] G. Calderini,[55] J. Chauveau,[55] O. Hamon,[55] Ph. Leruste,[55] G. Marchiori,[55] J. Ocariz,[55]
S. Sitt,[55] M. Biasini,[56a,56b] E. Manoni,[56a,56b] S. Pacetti,[56a,56b] A. Rossi,[56a,56b] C. Angelini,[57a,57b] G. Batignani,[57a,57b]
S. Bettarini,[57a,57b] M. Carpinelli,[57a,57b,¶] G. Casarosa,[57a,57b] A. Cervelli,[57a,57b] F. Forti,[57a,57b] M. A. Giorgi,[57a,57b]
A. Lusiani,[57a,57c] B. Oberhof,[57a,57b] E. Paoloni,[57a,57b] A. Perez,[57a] G. Rizzo,[57a,57b] J. J. Walsh,[57a] D. Lopes Pegna,[58]
J. Olsen,[58] A. J. S. Smith,[58] A. V. Telnov,[58] F. Anulli,[59a] R. Faccini,[59a,59b] F. Ferrarotto,[59a] F. Ferroni,[59a,59b]
M. Gaspero,[59a,59b] L. Li Gioi,[59a] M. A. Mazzoni,[59a] G. Piredda,[59a] C. Bünger,[60] O. Grünberg,[60] T. Hartmann,[60]
T. Leddig,[60] H. Schröder,[60,§] C. Voss,[60] R. Waldi,[60] T. Adye,[61] E. O. Olaiya,[61] F. F. Wilson,[61] S. Emery,[62]
G. Hamel de Monchenault,[62] G. Vasseur,[62] Ch. Yèche,[62] D. Aston,[63] D. J. Bard,[63] R. Bartoldus,[63] J. F. Benitez,[63]
C. Cartaro,[63] M. R. Convery,[63] J. Dorfan,[63] G. P. Dubois-Felsmann,[63] W. Dunwoodie,[63] M. Ebert,[63] R. C. Field,[63]
M. Franco Sevilla,[63] B. G. Fulsom,[63] A. M. Gabareen,[63] M. T. Graham,[63] P. Grenier,[63] C. Hast,[63] W. R. Innes,[63]
M. H. Kelsey,[63] P. Kim,[63] M. L. Kocian,[63] D. W. G. S. Leith,[63] P. Lewis,[63] B. Lindquist,[63] S. Luitz,[63] V. Luth,[63]
H. L. Lynch,[63] D. B. MacFarlane,[63] D. R. Muller,[63] H. Neal,[63] S. Nelson,[63] M. Perl,[63] T. Pulliam,[63] B. N. Ratcliff,[63]
A. Roodman,[63] A. A. Salnikov,[63] R. H. Schindler,[63] A. Snyder,[63] D. Su,[63] M. K. Sullivan,[63] J. Va'vra,[63] A. P. Wagner,[63]
W. J. Wisniewski,[63] M. Wittgen,[63] D. H. Wright,[63] H. W. Wulsin,[63] C. C. Young,[63] V. Ziegler,[63] W. Park,[64] M. V. Purohit,[64]
R. M. White,[64] J. R. Wilson,[64] A. Randle-Conde,[65] S. J. Sekula,[65] M. Bellis,[66] P. R. Burchat,[66] T. S. Miyashita,[66]
M. S. Alam,[67] J. A. Ernst,[67] R. Gorodeisky,[68] N. Guttman,[68] D. R. Peimer,[68] A. Soffer,[68] P. Lund,[69] S. M. Spanier,[69]
J. L. Ritchie,[70] A. M. Ruland,[70] R. F. Schwitters,[70] B. C. Wray,[70] J. M. Izen,[71] X. C. Lou,[71] F. Bianchi,[72a,72b]
D. Gamba,[72a,72b] L. Lanceri,[73a,73b] L. Vitale,[73a,73b] F. Martinez-Vidal,[74] A. Oyanguren,[74] H. Ahmed,[75] J. Albert,[75]
Sw. Banerjee,[75] F. U. Bernlochner,[75] H. H. F. Choi,[75] G. J. King,[75] R. Kowalewski,[75] M. J. Lewczuk,[75] I. M. Nugent,[75]
J. M. Roney,[75] R. J. Sobie,[75] N. Tasneem,[75] T. J. Gershon,[76] P. F. Harrison,[76] T. E. Latham,[76] E. M. T. Puccio,[76]
H. R. Band,[77] S. Dasu,[77] Y. Pan,[77] R. Prepost,[77] and S. L. Wu[77]

(B*A*B*AR* Collaboration)

[1]*Laboratoire d'Annecy-le-Vieux de Physique des Particules (LAPP), Université de Savoie, CNRS/IN2P3,*
F-74941 Annecy-Le-Vieux, France
[2]*Universitat de Barcelona, Facultat de Fisica, Departament ECM, E-08028 Barcelona, Spain*
[3a]*INFN Sezione di Bari, I-70126 Bari, Italy*
[3b]*Dipartimento di Fisica, Università di Bari, I-70126 Bari, Italy*
[4]*University of Bergen, Institute of Physics, N-5007 Bergen, Norway*
[5]*Lawrence Berkeley National Laboratory and University of California, Berkeley, California 94720, USA*
[6]*Ruhr Universität Bochum, Institut für Experimentalphysik 1, D-44780 Bochum, Germany*
[7]*University of British Columbia, Vancouver, British Columbia, Canada V6T 1Z1*
[8]*Brunel University, Uxbridge, Middlesex UB8 3PH, United Kingdom*
[9]*Budker Institute of Nuclear Physics, Novosibirsk 630090, Russia*
[10]*University of California at Irvine, Irvine, California 92697, USA*
[11]*University of California at Riverside, Riverside, California 92521, USA*
[12].*University of California at Santa Barbara, Santa Barbara, California 93106, USA*
[13]*University of California at Santa Cruz, Institute for Particle Physics, Santa Cruz, California 95064, USA*
[14]*California Institute of Technology, Pasadena, California 91125, USA*
[15]*University of Cincinnati, Cincinnati, Ohio 45221, USA*
[16]*University of Colorado, Boulder, Colorado 80309, USA*
[17]*Colorado State University, Fort Collins, Colorado 80523, USA*
[18]*Technische Universität Dortmund, Fakultät Physik, D-44221 Dortmund, Germany*
[19]*Technische Universität Dresden, Institut für Kern- und Teilchenphysik, D-01062 Dresden, Germany*
[20]*Laboratoire Leprince-Ringuet, Ecole Polytechnique, CNRS/IN2P3, F-91128 Palaiseau, France*
[21]*University of Edinburgh, Edinburgh EH9 3JZ, United Kingdom*
[22a]*INFN Sezione di Ferrara, I-44100 Ferrara, Italy*
[a22b]*Dipartimento di Fisica, Università di Ferrara, I-44100 Ferrara, Italy*
[23]*INFN Laboratori Nazionali di Frascati, I-00044 Frascati, Italy*
[24a]*INFN Sezione di Genova, I-16146 Genova, Italy*
[24b]*Dipartimento di Fisica, Università di Genova, I-16146 Genova, Italy*
[25]*Indian Institute of Technology Guwahati, Guwahati, Assam, 781 039, India*
[26]*Harvard University, Cambridge, Massachusetts 02138, USA*
[27]*Harvey Mudd College, Claremont, California 91711, USA*
[28]*Universität Heidelberg, Physikalisches Institut, Philosophenweg 12, D-69120 Heidelberg, Germany*
[29]*Humboldt-Universität zu Berlin, Institut für Physik, Newtonstrasse 15, D-12489 Berlin, Germany*
[30]*Imperial College London, London, SW7 2AZ, United Kingdom*
[31]*University of Iowa, Iowa City, Iowa 52242, USA*
[32]*Iowa State University, Ames, Iowa 50011-3160, USA*
[33]*Johns Hopkins University, Baltimore, Maryland 21218, USA*
[34]*Laboratoire de l'Accélérateur Linéaire, IN2P3/CNRS et Université Paris-Sud 11, Centre Scientifique d'Orsay,*
B. P. 34, F-91898 Orsay Cedex, France
[35]*Lawrence Livermore National Laboratory, Livermore, California 94550, USA*
[36]*University of Liverpool, Liverpool L69 7ZE, United Kingdom*
[37]*Queen Mary, University of London, London, E1 4NS, United Kingdom*
[38]*University of London, Royal Holloway and Bedford New College, Egham, Surrey TW20 0EX, United Kingdom*
[39]*University of Louisville, Louisville, Kentucky 40292, USA*
[40]*Johannes Gutenberg-Universität Mainz, Institut für Kernphysik, D-55099 Mainz, Germany*
[41]*University of Manchester, Manchester M13 9PL, United Kingdom*
[42]*University of Maryland, College Park, Maryland 20742, USA*
[43]*University of Massachusetts, Amherst, Massachusetts 01003, USA*
[44]*Massachusetts Institute of Technology, Laboratory for Nuclear Science, Cambridge, Massachusetts 02139, USA*
[45]*McGill University, Montréal, Québec, Canada H3A 2T8*
[46a]*INFN Sezione di Milano, I-20133 Milano, Italy*
[46b]*Dipartimento di Fisica, Università di Milano, I-20133 Milano, Italy*
[47]*University of Mississippi, University, Mississippi 38677, USA*
[48]*Université de Montréal, Physique des Particules, Montréal, Québec, Canada H3C 3J7*
[49a]*INFN Sezione di Napoli, I-80126 Napoli, Italy*
[49b]*Dipartimento di Scienze Fisiche, Università di Napoli Federico II, I-80126 Napoli, Italy*
[50]*NIKHEF, National Institute for Nuclear Physics and High Energy Physics, NL-1009 DB Amsterdam, Netherlands*

^{51}*University of Notre Dame, Notre Dame, Indiana 46556, USA*

^{52}*Ohio State University, Columbus, Ohio 43210, USA*

^{53}*University of Oregon, Eugene, Oregon 97403, USA*

^{54a}*INFN Sezione di Padova, I-35131 Padova, Italy*

^{54b}*Dipartimento di Fisica, Università di Padova, I-35131 Padova, Italy*

^{55}*Laboratoire de Physique Nucléaire et de Hautes Energies, IN2P3/CNRS, Université Pierre et Marie Curie-Paris6,*

Université Denis Diderot-Paris7, F-75252 Paris, France

^{56a}*INFN Sezione di Perugia, I-06100 Perugia, Italy*

^{56b}*Dipartimento di Fisica, Università di Perugia, I-06100 Perugia, Italy*

^{57a}*INFN Sezione di Pisa, I-56127 Pisa, Italy*

^{57b}*Dipartimento di Fisica, Università di Pisa, I-56127 Pisa, Italy*

^{57c}*Scuola Normale Superiore di Pisa, I-56127 Pisa, Italy*

^{58}*Princeton University, Princeton, New Jersey 08544, USA*

^{59a}*INFN Sezione di Roma, I-00185 Roma, Italy*

^{59b}*Dipartimento di Fisica, Università di Roma La Sapienza, I-00185 Roma, Italy*

^{60}*Universität Rostock, D-18051 Rostock, Germany*

^{61}*Rutherford Appleton Laboratory, Chilton, Didcot, Oxon, OX11 0QX, United Kingdom*

^{62}*CEA, Irfu, SPP, Centre de Saclay, F-91191 Gif-sur-Yvette, France*

^{63}*SLAC National Accelerator Laboratory, Stanford, California 94309, USA*

^{64}*University of South Carolina, Columbia, South Carolina 29208, USA*

^{65}*Southern Methodist University, Dallas, Texas 75275, USA*

^{66}*Stanford University, Stanford, California 94305-4060, USA*

^{67}*State University of New York, Albany, New York 12222, USA*

^{68}*Tel Aviv University, School of Physics and Astronomy, Tel Aviv, 69978, Israel*

^{69}*University of Tennessee, Knoxville, Tennessee 37996, USA*

^{70}*University of Texas at Austin, Austin, Texas 78712, USA*

^{71}*University of Texas at Dallas, Richardson, Texas 75083, USA*

^{72a}*INFN Sezione di Torino, I-10125 Torino, Italy*

^{72b}*Dipartimento di Fisica Sperimentale, Università di Torino, I-10125 Torino, Italy*

^{73a}*INFN Sezione di Trieste, I-34127 Trieste, Italy*

^{73b}*Dipartimento di Fisica, Università di Trieste, I-34127 Trieste, Italy*

^{74}*IFIC, Universitat de Valencia-CSIC, E-46071 Valencia, Spain*

^{75}*University of Victoria, Victoria, British Columbia, Canada V8W 3P6*

^{76}*Department of Physics, University of Warwick, Coventry CV4 7AL, United Kingdom*

^{77}*University of Wisconsin, Madison, Wisconsin 53706, USA*

We report the measurement of the baryonic *B* decay $B^- \to \Sigma_c^{++} \bar{p} \pi^- \pi^-$. Using a data sample of 467×10^6 $B\bar{B}$ pairs collected with the *BABAR* detector at the PEP-II storage ring at SLAC, the measured branching fraction is $(2.98 \pm 0.16_{\text{(stat)}} \pm 0.15_{\text{(syst)}} \pm 0.77_{(\Lambda_c)}) \times 10^{-4}$, where the last error is due to the uncertainty in $\mathcal{B}(\Lambda_c^+ \to pK^- \pi^+)$. The data suggest the existence of resonant subchannels $B^- \to \Lambda_c(2595)^+ \bar{p} \pi^-$ and, possibly, $B^- \to \Sigma_c^{++} \bar{\Delta}^{--} \pi^-$. We see unexplained structures in $m(\Sigma_c^{++} \pi^- \pi^-)$ at 3.25 GeV/c^2, 3.8 GeV/c^2, and 4.2 GeV/c^2.

I. INTRODUCTION

The large mass of the *B* meson allows a wide spectrum of baryonic decays, which have, in total, a

*Now at the University of Tabuk, Tabuk 71491, Saudi Arabia.

†Also with Università di Perugia, Dipartimento di Fisica, Perugia, Italy.

‡Now at the University of Huddersfield, Huddersfield HD1 3DH, UK.

§Deceased.

$^\|$Now at University of South Alabama, Mobile, AL 36688, USA.

¶Also with Università di Sassari, Sassari, Italy.

branching fraction of $(6.8 \pm 0.6)\%$ [1]. This makes *B* decays a good place to study the mechanisms of baryon production. One approach to investigate the baryonization process in *B* decays is to measure and compare their exclusive branching fractions and study the dynamic structure of the decay, i.e., the influence of resonant subchannels.

In this paper, we present a study of the decay $B^- \to \Sigma_c^{++} \bar{p} \pi^- \pi^-$ [2]. This decay is a resonant subchannel of the five-body final state $B^- \to \Lambda_c^+ \bar{p} \pi^+ \pi^- \pi^-$, which has the largest hitherto known branching fraction among all baryonic *B* decays and hence is a good starting point for further investigations. The analyzed decay can be

compared with $B^- \to \Sigma_c^0 \bar{p} \pi^+ \pi^-$ and $\bar{B}^0 \to \Sigma_c^{++} \bar{p} \pi^-$, which have similar quark content and phase space.

Large differences between the branching fractions of $B^- \to \Sigma_c^{++} \bar{p} \pi^- \pi^-$, $B^- \to \Sigma_c^0 \bar{p} \pi^+ \pi^-$, and $\bar{B}^0 \to \Sigma_c^{++} \bar{p} \pi^-$ could indicate a considerable impact of intermediate states on baryonic B decays. For example, the decay $B^- \to \Sigma_c^0 \bar{p} \pi^+ \pi^-$ allows a number of resonant three-body decays (including $\bar{N}$, $\bar{\Delta}^0$, and ρ^0 resonances) that cannot occur in $B^- \to \Sigma_c^{++} \bar{p} \pi^- \pi^-$. The importance of resonant subchannels can be quantified, e.g., by the ratio of $[\mathcal{B}(B^- \to \Sigma_c^{++} \bar{p} \pi^- \pi^-) + \mathcal{B}(B^- \to \Sigma_c^0 \bar{p} \pi^+ \pi^-)]/ \mathcal{B}(B^- \to \Lambda_c^+ \bar{p} \pi^+ \pi^- \pi^-)$.

The CLEO Collaboration measured $\mathcal{B}(B^- \to \Lambda_c^+ \bar{p} \pi^+ \pi^- \pi^-) = (22.5 \pm 3.5 \pm 5.8) \times 10^{-4}$ and $\mathcal{B}(B^- \to \Sigma_c^0 \bar{p} \pi^+ \pi^-) = (4.4 \pm 1.7 \pm 1.1) \times 10^{-4}$ [3]. The decay $\bar{B}^0 \to \Sigma_c^{++} \bar{p} \pi^-$ was measured by the CLEO [3] and the Belle [4] Collaborations. The Particle Data Group has calculated an average of $\mathcal{B}(\bar{B}^0 \to \Sigma_c^{++} \bar{p} \pi^-) = (2.2 \pm 0.7 \pm 0.6) \times 10^{-4}$ [1]. For all these branching fractions the first uncertainty is the combined statistical and systematic error, and the second one is due to the uncertainty in $\mathcal{B}(\Lambda_c^+ \to pK^- \pi^+) = (5.0 \pm 1.3)\%$ [1].

II. THE *BABAR* EXPERIMENT

This analysis is based on a data set of about 426 fb^{-1}, corresponding to 467×10^6 $B\bar{B}$ pairs. The sample was collected with the *BABAR* detector at the PEP-II asymmetric-energy $e^+ e^-$ storage ring, which was operated at a center-of-mass energy equal to the $\Upsilon(4S)$ mass. For generation of Monte Carlo (MC) simulated data we use EVTGEN [5] for event generation and GEANT4 [6] for detector simulation.

The *BABAR* detector is described in detail elsewhere [7]. The selection of proton, kaon, and pion candidates is based on measurements of the energy loss in the silicon vertex tracker and the drift chamber, and of the Cherenkov radiation in the detector of internally reflected Cherenkov light [8]. The average efficiency for pion identification is approximately 95%, with a typical misidentification rate of 10% due to other charged particles such as muons and kaons, depending on the momentum and the polar angle of the particle. The efficiency for kaon identification is about 95% with a misidentification rate less than 5% due to protons and pions. The efficiency for proton and antiproton identification is about 90% with a misidentification rate about 2% due to kaons.

III. DECAY RECONSTRUCTION

The decay $B^- \to \Sigma_c^{++} \bar{p} \pi^- \pi^-$ is reconstructed in the subchannel $\Sigma_c^{++} \to \Lambda_c^+ \pi^+$, $\Lambda_c^+ \to pK^- \pi^+$. For the reconstruction of the B candidate the entire decay tree is fitted simultaneously. A vertex fit is performed for B^-, Σ_c^{++}, and Λ_c^+, and the χ^2 fit probability is required to exceed 0.1%.

To suppress background, the invariant mass of the $pK^- \pi^+$ combination is required to satisfy $2275 \text{ MeV}/c^2 < m_{pK^- \pi^+} < 2296 \text{ MeV}/c^2$, i.e., compatible with coming from the decay $\Lambda_c^+ \to pK^- \pi^+$. This selection corresponds to 2.8 times the observed width of reconstructed Λ_c^+ candidates, which are centered at $m_{pK^- \pi^+} = 2285.4 \text{ MeV}/c^2$. The separation of signal from background in the B-candidate sample is obtained using two kinematic variables, $\Delta E = E_B^* - \sqrt{s}/2$ and $m_{\text{ES}} = \sqrt{(s/2 + \mathbf{p}_i \cdot \mathbf{p}_B)^2/E_i^2 - |\mathbf{p}_B|^2}$, where $\sqrt{s}$ is the center-of-mass (CM) energy of the $e^+ e^-$ pair and E_B^* the energy of the B candidate in the CM system. $(E_i, \mathbf{p}_i)$ is the four-momentum vector of the $e^+ e^-$ CM system and $\mathbf{p}_B$ the B-candidate momentum vector, both measured in the laboratory frame. For correctly reconstructed B decays, m_{ES} is centered at the B meson mass and ΔE is centered at zero. Throughout this analysis, B candidates are required to have m_{ES} within 8 MeV (3.4σ) of the measured B mass of $m_{\text{ES}} = 5279.1 \text{ MeV}$.

Figure 1 shows the distribution of $\Delta M \equiv m(\Lambda_c^+ \pi^+) - m(\Lambda_c^+)$ in data for candidates that satisfy the criteria described above for m_{ES} and $m_{pK^- \pi^+}$ and for which ΔE is between -60 MeV and $+40$ MeV. We perform a binned minimum χ^2 fit using a second-order polynomial for the description of the background and the sum of a Voigt distribution (the convolution of a Breit-Wigner function with a Gaussian function) and a Gaussian to parametrize the Σ_c^{++} signal. A detailed explanation of the fit function is given in Sec. IV. The fitted Σ_c^{++} signal yield is $N = 1020 \pm 95$.

Figure 2 shows the ΔE distribution in data for candidates that satisfy the criteria described above for m_{ES} and $m_{pK^- \pi^+}$ and for which ΔM is between 0.157 GeV/c^2 and 0.178 GeV/c^2. The latter is a selection of Σ_c^{++} candidates with an efficiency of 92% in signal MC data.
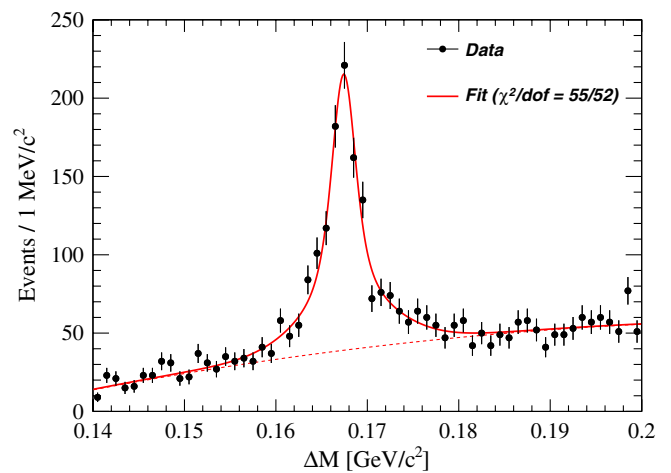

FIG. 1 (color online). Fitted ΔM distribution for B candidates in data. All candidates are required to satisfy the selection criteria on m_{ES}, $m_{pK^- \pi^+}$, and ΔE.
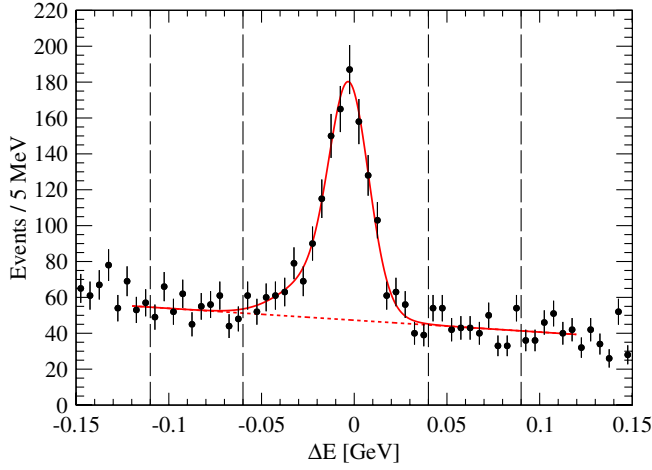
FIG. 2 (color online). Fitted ΔE distribution in data with selection criteria applied to $m_{pK^-\pi^+}$, m_{ES}, and ΔM. The goodness of the fit is $\chi^2/\mathrm{dof} = 36/40$. The ΔE signal region is between -60 MeV and 40 MeV and is enclosed by the two sideband regions that each have a width of 50 MeV.

In the binned minimum χ^2 fit we use the sum of two Gaussian functions for the signal and a linear function for the background. The second Gaussian accommodates B decays with missing energy due to final state radiation. Each Gaussian has a mean parameter (μ) and a standard deviation (σ). The joint normalization is described by N_{sig} and the fraction of the first Gaussian is f_1. We parametrize the background shape of the ΔE distribution as a first-order polynomial, which provides a good description of the ΔE distribution for candidates in the m_{ES} sideband in the range $5.20\ \mathrm{GeV}/c^2 < m_{\mathrm{ES}} < 5.26\ \mathrm{GeV}/c^2$. All parameters are permitted to vary during fitting. Table I presents the resulting signal parameters. The signal yield is 840 ± 55 events.

IV. SIGNAL EXTRACTION

There are two sources of background that contribute to the signal in ΔE and ΔM. The first one is B decays that have the same final state, in particular $B^- \rightarrow \Lambda_c^+ \bar{p} \pi^+ \pi^- \pi^-$, and the other one is B decays that have a Σ_c^{++} among its decay products, e.g., $\bar{B}^0 \rightarrow \Sigma_c^{++} \bar{p} \pi^- \pi^0$. To reject this background, we make a binwise fit using ΔM as a discriminating

TABLE I. The parameters for the double-Gaussian function describing the signal contribution in the fit to the ΔE distribution shown in Fig. 2. f_1 is the fraction of the signal in the narrower Gaussian.

Parameter	Fit result
N_{sig}	840 ± 55
f_1	$(70 \pm 23)\%$
μ_1	(-2.7 ± 1.2) MeV
σ_1	(10 ± 1.6) MeV
μ_2	(-16 ± 14) MeV
σ_2	(20 ± 5.6) MeV

variable to create a background-subtracted ΔE distribution from which we extract the true signal yield in order to determine $\mathcal{B}(B^- \rightarrow \Sigma_c^{++} \bar{p} \pi^- \pi^-)$. The binwise fitting procedure is described in the following paragraph.

After applying the selection in $m_{pK^-\pi^+}$ and m_{ES} (no selection in ΔM), we divide the ΔE range $(-105, 105)$ MeV into 14 equal slices and fit the ΔM distribution in each slice separately in the range $0.14\ \mathrm{GeV}/c^2 < \Delta M < 0.2\ \mathrm{GeV}/c^2$. In the fits the Σ_c^{++} signal is represented by the sum of a Voigt function and a Gaussian function. The Voigt distribution has four parameters ($N_{\mathrm{sig}}, \mu, \Gamma, \sigma$) and models the signal peak region, where μ is the mean of the Voigt and represents the Σ_c^{++} mass, which is fixed to the value obtained from an inclusive analysis of $\Sigma_c^{++} \rightarrow \Lambda_c^+ \pi^+$ candidates in the data. The parameter Γ is the intrinsic width of the Σ_c^{++} and is fixed to the 2010 Review of Particle Properties (RPP) value [1], and σ describes the detector resolution in ΔM for the Σ_c^{++} determined, independently for each ΔE slice, from the signal MC data. The remaining parameter N_{sig}^i is the fitted Σ_c^{++} signal yield in each of the ΔE bins.

There is a correlation between ΔM and ΔE that is very prominent due to the inaccurate momentum measurement of the slow π^+ from the Σ_c^{++} decay. As a result the Σ_c^{++} signal has tails in the ΔM distribution that are modeled by the Gaussian function whose parameters are determined, independently for each ΔE slice, from the signal MC data. The background is represented by a second-order polynomial. This shape was determined from the sidebands $|\Delta E| \in (50, 300)$ MeV and, compared to the other polynomials, gives the best χ^2 fit probability. The fits in ΔM determine the background level and the number of Σ_c^{++} baryons.

Figure 3 shows the Σ_c^{++} signal yield as a function of ΔE. We fit this distribution with the same functions described in
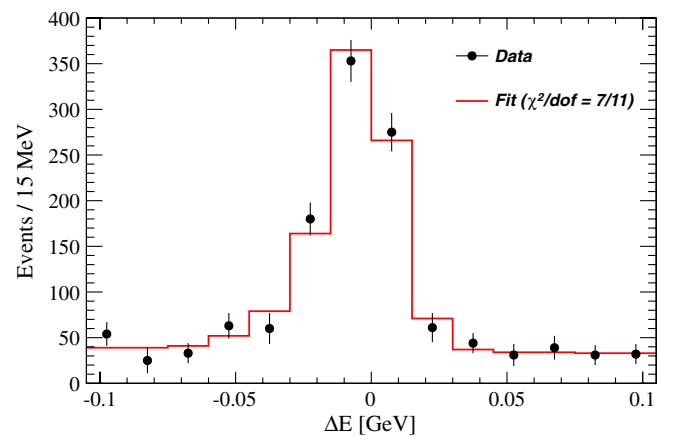

FIG. 3 (color online). ΔE distribution for $B^- \rightarrow \Sigma_c^{++} \bar{p} \pi^- \pi^-$ candidates in data. The points with error bars represent the number of Σ_c^{++} candidates N_{sig}^i from a fit to $\Delta M \equiv m(\Lambda_c^+ \pi^+) - m(\Lambda_c^+)$. All signal parameters for the ΔE distribution, except N_{sig}, are fixed to those shown in Table I.

Sec. III and fix the signal parameters, except for N_{sig}, to those determined there. The true signal yield is $N_{\text{sig}} = 787 \pm 43$ events.

V. EFFICIENCY

The efficiency is calculated from the simulated events. These events were generated uniformly in four-body phase space (PS), but the actual decay distribution is, *a priori*, unknown. Therefore, when calculating the efficiency, we weight the MC events so that we reproduce the distributions of the two-body invariant mass distributions for the decay products of the B candidates in data. The resulting efficiency is checked by repeating the procedure using the three-body masses and then again using the angles between the B daughters in the B rest frame. The different procedures give an average efficiency of $(11.3 \pm 0.2_{\text{(syst)}})\%$, which is used to determine the branching fraction. Out of the efficiencies from the different procedures, we use the maximum deviation from the average efficiency as systematic uncertainty. The statistical uncertainty, due to the use of the data, is negligible compared to the statistical uncertainty in the event yield. The efficiency calculated using unweighted events is 11.0%.

VI. SYSTEMATIC UNCERTAINTIES

We estimate the uncertainty on the signal extraction in three different ways: (1) the fit to ΔE in Fig. 3 is repeated separately for each shape parameter in Table I, while permitting this parameter to float. The absolute deviations (δN) in the event yield to our true signal yield $N_{\text{sig}} = 787$

TABLE II. The results of the fits to ΔE in Fig. 3 while the given parameter is allowed to float. δN is the absolute deviation to our true signal yield $N_{\text{sig}} = 787$.

Floating parameter	Fit result	δN
f_1	$(70 \pm 7.7)\%$	2
μ_1	(-2.8 ± 1.0) MeV	0
σ_1	(11 ± 0.9) MeV	8
μ_2	(-15 ± 5.2) MeV	2
σ_2	(18 ± 4.6) MeV	11

add up to 23 (see Table II). (2) We use a second-order polynomial for the background while letting all other parameters fixed ($\delta N = 5$), and (3) we fit only the background with a first-order polynomial and subtract its integral from the histogram content in the range $-60 \text{ MeV} < \Delta E < 45 \text{ MeV}$ in order to obtain an alternative signal yield ($\delta N = 3$). The absolute values of the deviations in the event yields from all of these variations add up to 31. The resulting relative uncertainty on the signal yield is 4.0%. Other systematic errors come from track reconstruction efficiency (2.4%) [9], efficiency (1.8%), and the number of produced $B\bar{B}$ pairs in the data sample (1.1%). The total relative uncertainty on the branching fraction is 5.1%.

VII. BRANCHING FRACTION RESULTS

Using the results from the signal extraction, efficiency determination, and estimation of systematic errors, we find

$$\mathcal{B}(B^- \to \Sigma_c^{++} \bar{p} \pi^- \pi^-) \cdot \mathcal{B}(\Lambda_c^+ \to pK^- \pi^+) = \frac{N_{\text{sig}}}{\varepsilon \cdot N_{B\bar{B}}} = (1.49 \pm 0.08_{\text{(stat)}} \pm 0.08_{\text{(syst)}}) \times 10^{-5}, \quad (1)$$

$$\mathcal{B}(B^- \to \Sigma_c^{++} \bar{p} \pi^- \pi^-) = \frac{N_{\text{sig}}}{\varepsilon \cdot N_{B\bar{B}} \cdot \mathcal{B}(\Lambda_c^+ \to pK^- \pi^+)} = (2.98 \pm 0.16_{\text{(stat)}} \pm 0.15_{\text{(syst)}} \pm 0.77_{(\Lambda_c)}) \times 10^{-4}. \quad (2)$$

In Eq. (2) the last error is due to the uncertainty in $\mathcal{B}(\Lambda_c^+ \to pK^- \pi^+)$.

VIII. FRACTION OF PS DISTRIBUTED DECAYS

To compare the two-body and three-body invariant masses of the B decay products in data with PS, we determine an effective PS fraction of the total branching ratio. To do this, we assume that the resonant substructures are due to the intermediate states $\Lambda_c^{*+} \to \Sigma_c^{++} \pi^-$ and $\bar{\Delta}^{--} \to \bar{p} \pi^-$, and the remainder is distributed according to four-body PS. We investigate all two-dimensional planes that are spanned by the two-body invariant masses of the B decay products, e.g. $m(\Sigma_c^{++} \pi_s^-)$ against $m(\bar{p}\pi_f^-)$, to look for a range that is free from Λ_c^{*+} and $\bar{\Delta}^{--}$ resonances and hence can be described by a four-body PS distribution. The symbol

π_s^- refers to the π^- that has the lower momentum in the $e^+ e^-$ CM system. The other π^- is denoted as π_f^-. We see no indication of $\bar{\Delta}^{--}$ and Λ_c^{*+} resonances for B candidates in the range $3.050 \text{ GeV}/c^2 < m(\Sigma_c^{++} \pi_s^-) < 3.450 \text{ GeV}/c^2$, where the normalization of the PS distribution is determined by fitting the sideband-subtracted data (Fig. 4).

From the ratio of the efficiency-corrected integrals of the distributions in Fig. 4, we calculate an effective PS fraction:

$$\frac{\mathcal{B}(B^- \to \Sigma_c^{++} \bar{p} \pi^- \pi^-)_{\text{PS}}}{\mathcal{B}(B^- \to \Sigma_c^{++} \bar{p} \pi^- \pi^-)} = \frac{389}{11.0\%} \cdot \frac{11.3\%}{816} = 49\%. \quad (3)$$

This percentage will be used to normalize the PS projection in the two-body and three-body invariant mass distributions in Figs. 5–7.
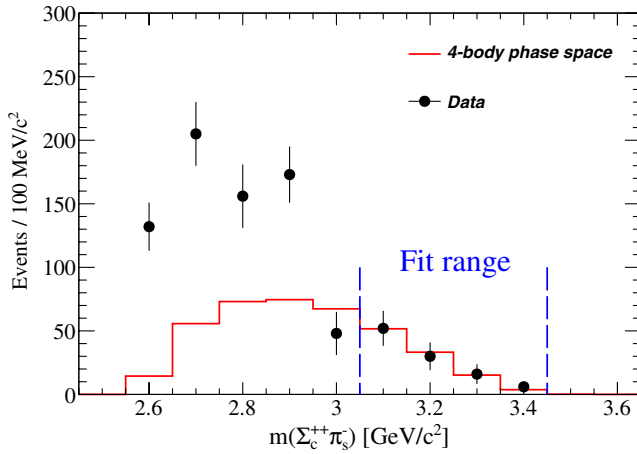
FIG. 4 (color online). The $m(\Sigma_c^{++}\pi_s^-)$ distribution in data (points with error bars) and for simulated four-body phase space decays (histogram). The distribution in data results from a sideband subtraction in ΔE according to the definition in Fig. 2.

IX. RESONANT SUBCHANNELS

Figure 5 shows the invariant mass distribution of $\bar{p}\pi^- = \{\bar{p}\pi_s^-, \bar{p}\pi_f^-\}$ [sum of the distributions of $m(\bar{p}\pi_s^-)$ and $m(\bar{p}\pi_f^-)$] after sideband subtraction in ΔE (see Fig. 2 for the definition of the sidebands) and efficiency correction. The efficiency correction here and in the other invariant masses of the *B* daughters is determined from PS MC data for the particular mass that is considered. The differences between data and PS in the range $m(\bar{p}\pi^-) \in (1.2, 1.7)$ GeV/c^2 are compatible with the existence of the resonances $\bar{\Delta}^{--}(1232, 1600, 1620)$.

Figure 6 shows the invariant mass of $\Sigma_c^{++}\pi^- = \{\Sigma_c^{++}\pi_s^-, \Sigma_c^{++}\pi_f^-\}$ after efficiency correction and sideband subtraction in ΔE. The large number of events at threshold
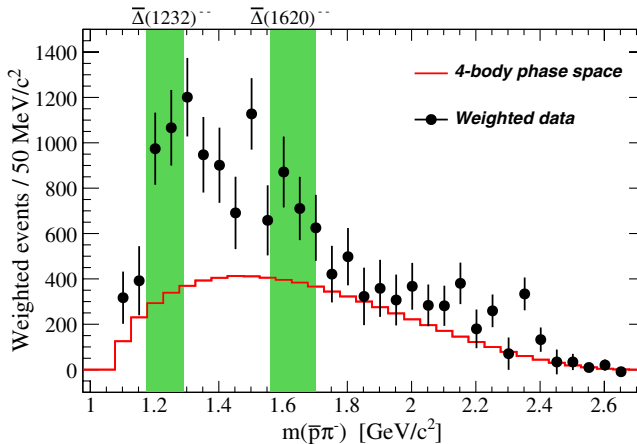

FIG. 5 (color online). The $m(\bar{p}\pi^-)$ distribution in data and simulated four-body phase space decays. The shaded vertical ranges represent a width of one Γ and are centered at the average mass of $\bar{\Delta}^{--}(1232)$ and $\bar{\Delta}^{--}(1620)$, respectively. The parameters are taken from the RPP [1]. The range of $\bar{\Delta}^{--}(1600)$ is not drawn since its parameters have large uncertainties.
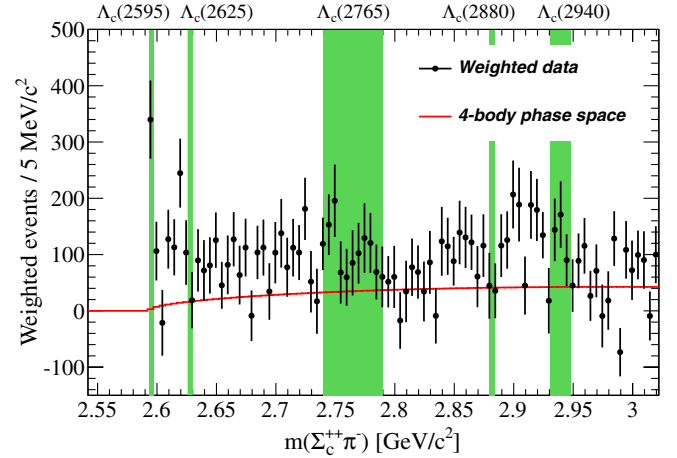

FIG. 6 (color online). The $m(\Sigma_c^{++}\pi^-)$ distribution in data after efficiency correction and ΔE-sideband subtraction. The solid line shows four-body phase space decays. The shaded vertical ranges represent a width of one Γ and are centered at the average mass of the respective Λ_c^{*+} resonance. The parameters are taken from the RPP [1].
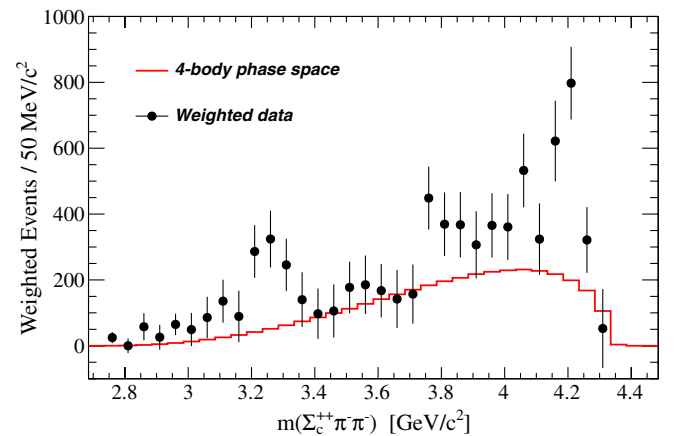

FIG. 7 (color online). The $m(\Sigma_c^{++}\pi^-\pi^-)$ distribution in data and simulated four-body phase space decays. The histogram in data includes efficiency correction and ΔE-sideband subtraction according to the definition in Fig. 2.

are consistent with the decay $B^- \to \Lambda_c(2595)^+\bar{p}\pi^-$. There are no significant signals for other Λ_c^{*+} resonances.

In the three-body invariant mass distribution $m(\Sigma_c^{++}\pi^-\pi^-)$ (Fig. 7) we see unexplained structures at 3.25 GeV/c^2, 3.8 GeV/c^2, and 4.2 GeV/c^2. However, because of the limited number of signal candidates, it is not possible to analyze these enhancements in more detail.

We find no indication of a threshold enhancement in the baryon-antibaryon mass distribution.

X. SUMMARY AND CONCLUSIONS

We have measured the branching fraction $\mathcal{B}(B^- \to \Sigma_c^{++}\bar{p}\pi^-\pi^-) = (2.98 \pm 0.22 \pm 0.77_{(\Lambda_c)}) \times 10^{-4}$. This improves on the previous measurement by CLEO [3].

We have calculated an effective PS fraction of 49% for the observed decay, which may indicate the importance of resonant substructures in baryonic B decays. By comparing the data and four-body PS in the distributions of the invariant masses of the B daughters, we find suggestions for the resonant subchannels $B^- \to \Lambda_c(2595)^+ \bar{p} \pi^-$ and, possibly, $B^- \to \Sigma_c^{++} \bar{\Delta}^{--} \pi^-$. Additionally, we see unexplained structures in $m(\Sigma_c^{++} \pi^- \pi^-)$ at 3.25 GeV/c^2, 3.8 GeV/c^2, and 4.2 GeV/c^2.

Combining our measurement with the results $\mathcal{B}(B^- \to \Sigma_c^0 \bar{p} \pi^+ \pi^-) = (4.4 \pm 2.0) \times 10^{-4}$ and $\mathcal{B}(B^- \to \Lambda_c^+ \bar{p} \pi^+ \pi^- \pi^-) = (22.5 \pm 6.8) \times 10^{-4}$ from CLEO [3], we calculate the resonant fractions $\frac{\mathcal{B}(B^- \to \Sigma_c^{++} \bar{p} \pi^- \pi^-)}{\mathcal{B}(B^- \to \Lambda_c^+ \bar{p} \pi^+ \pi^- \pi^-)} = (13.2 \pm 4.1)\%$ and $\frac{\mathcal{B}(B^- \to \Sigma_c^{++} \bar{p} \pi^- \pi^-) + \mathcal{B}(B^- \to \Sigma_c^0 \bar{p} \pi^+ \pi^-)}{\mathcal{B}(B^- \to \Lambda_c^+ \bar{p} \pi^+ \pi^- \pi^-)} = (33 \pm 13)\%$.

ACKNOWLEDGMENTS

[1] K. Nakamura *et al.* (Particle Data Group), J. Phys. G **37**, 075021 (2010).

[2] Throughout this paper, all decay modes represent that mode and its charge conjugate.

[3] S. A. Dytman *et al.* (CLEO Collaboration), Phys. Rev. D **66**, 091101 (2002).

[4] K. S. Park *et al.* (Belle Collaboration), Phys. Rev. D **75**, 011101 (2007).

[5] D. J. Lange, Nucl. Instrum. Methods Phys. Res., Sect. A **462**, 152 (2001).

[6] S. Agostinelli *et al.* (GEANT4 Collaboration), Nucl. Instrum. Methods Phys. Res., Sect. A **506**, 250 (2003).

[7] B. Aubert *et al.* (*BABAR* Collaboration), Nucl. Instrum. Methods Phys. Res., Sect. A **479**, 1 (2002).

[8] B. Aubert *et al.* (*BABAR* Collaboration), Phys. Rev. D **66**, 032003 (2002).

[9] T. Allmendinger *et al.*, arXiv:1207.2849 [Nucl. Instrum. Methods Phys. Res., Sect. A (to be published)].